Understanding the source-sink dynamics of PAHs at the sediment-water interface of a typical Karst wetland, southwest China

Weijie Liu [a, d], Xinli Xing [a, b]*; Xin, Li [a]; Yanqi Ma [a]; Cheng Cheng [a]; Mingming Shi [a]; Tianpeng Hu[c]; Andrew Sweetman [d]; Shihua Qi [a, b];

a, School of Environmental Studies, China University of Geosciences, Wuhan 430074, China

b, State Key Laboratory of Geomicrobiology and Environmental Changes, China University of Geosciences, Wuhan 430074, China

c, Hubei Key Laboratory of Mine Environmental Pollution Control and Remediation, School of Environmental Science and Engineering, Hubei Polytechnic University, Huangshi, 435003, China

d, Lancaster Environment Centre, Lancaster University, Lancaster, LA1 4YQ, UK

* To whom correspondence should be addressed Email: xlxing@cug.edu.cn ;

Abstract: Understanding the behavior and fate of PAHs in karst systems is crucial, as their distinctive geological features could facilitate rapid pollutant transport and complex source-sink dynamics. Previous studies have predominantly concentrated in PAHs transport at the sediment-water interface using fugacity theory, but these lack an integrated approach that couples multiple environmental factors to further quantify the source-sink transformation processes of PAHs. In this study, PAHs in sediment and water of a typical karst wetland were determined during both wet and dry seasons. Results suggest that average PAHs concentrations increased by 10.6% in water and by 46.0% in sediment from wet seasons to dry seasons. A

significant difference was also observed between the two seasonal source apportionments, suggesting that transport processes of PAHs in multiphase media should be integrated with source estimates. Increased secondary release potential of PAHs (3 rings and 4 rings) at the sediment-water interface was captured in dry seasons by both fugacity model and linear mixed effect models. PAHs transport was strongly affected by seasonal effects and the presence of labile organic carbon. From wet to dry seasons, PAHs in sediment shifted from acting a “sink” to “secondary source” as suggested by a Bayesian Gaussian regression and Bayesian network modeling. This study provides valuable insights into the source - sink dynamics processes of PAHs in a typical karst wetland.

Keywords: Polycyclic aromatic hydrocarbons; Huixian Wetland; Water-sediment exchange; Source-sink processes;

1. Introduction

Lakes serve as a critical role of aquatic ecosystems, contributing to water purification, climate regulation, and regional biodiversity conservation (Zhang et al., 2025a). Furthermore, lakes function as environmental geochemistry reactors, mediating the occurrence, transformation, and biogeochemical cycling of both nutrients (e.g., nitrogen and phosphorus) and organic contaminants (Dippong et al., 2024; Lahens et al., 2024). Importantly, pollutants that accumulate in lake sediment could undergo cycles of transport, deposition, and secondary release under changing environmental conditions (Jiang et al., 2022). Generally, pollutant source apportionment based on data from sediments or overlying water samples overlooks the changes resulting from their phase transport and fractionation effects, which could compromise

the effectiveness of pollution control strategies (Tobiszewski and Namiesnik, 2012). Therefore, it is essential to incorporate the redistribution dynamics of pollutants into source apportionment frameworks.

Polycyclic aromatic hydrocarbons (PAHs) are prevalent in lake systems raising concerns owing to their adverse effects (carcinogenic, teratogenic, and mutagenic) and high bioaccumulation potential (Sun et al., 2022). PAHs can be released into the environment by natural processes (volcanic eruptions, forest wildfires, and diagenesis) and anthropogenic activities (industrial combustion, residential coal combustion, biomass burning, vehicle emissions, and coking production) (Liu et al., 2025b; Xing et al., 2023). Previous studies have suggested that the latter was responsible for more than 90% of the annual emissions of PAHs (Shen et al., 2013). High levels of accumulation of PAHs (exceeded the United States Environmental Protection Agency guideline value, 200 $ng \cdot L^{-1}$) have been reported in lake water and sediments based on previous studies (Gong et al., 2022; Guo et al., 2012; Zhang et al., 2025a). Evidence suggests that PAHs contamination of lakes has shown significantly declines as a result of the implementation of stricter environmental regulations and improved pollution control measures (e.g., enhanced industrial emission standards and better wastewater treatment technologies) (Han and Currell, 2017; He et al., 2020). Nevertheless, residual PAHs in sediments and their secondary release potential suggest that continued monitoring and management are warranted.

A principle challenge in evaluating the transport and secondary release potential of PAHs from sediments is conducting sampling that accurately reflects the spatial and temporal

variability of complex aquatic environmental systems (Moran et al., 2024). Mackay (1979) developed a fugacity-based model to predict the distribution and transport of chemical pollutants across various environmental media under non-steady-state, non-equilibrium, and advective flow conditions (Lu et al., 2024). Mass balance fugacity models allow for the estimation of pollutant transport trends when parameterized appropriately (Zhang et al., 2025b). Although the transport flux, enrichment, and fate of PAHs can be quantified in lakes, the potential mechanisms of PAHs migration remain unclear. Generally, PAH transport is influenced by hydrodynamic conditions, presence of organic matter, hydro chemical composition and presence of multiple micropollutants (Liu et al., 2025b; Zhang et al., 2025a). In particular, organic carbon (OC) cycling in aquatic environments plays a critical role in governing the environmental fate of PAHs by via sorption, retention and remobilization (Nybom et al., 2024). Current studies, however, often consider OC as a bulk parameter, without distinguishing between its physiochemically distinct components under seasonally varying conditions. This limits our insight into the mechanisms by which different carbon fractions affect PAHs behavior in aquatic systems.

Karst lake wetlands systems have been characterized by unique hydrological and geological features, including soluble bedrock and high connectivity between surface water and groundwater, complicating the fate and transport of contaminants (Cheng et al., 2021; Li et al., 2024a). Recently, increasing attention has been given to the behavior of PAHs because the thin soil cover and high permeability typical of karst terrains could accelerate migration of contaminants and reduce natural attenuation capacity, especially at the sediment-water interface

(Luo et al., 2025; Miao et al., 2023). Accordingly, understanding the dynamics of PAH behavior in karst lake wetlands is of paramount importance for environmental management and sustainable development. This study aims to investigate the occurrence and spatial-temporal distribution of PAHs in a typical Karst wetland across seasons to enhance the accuracy of source quantification arising from fractionation and phase transport. This will help to elucidate the potential mechanisms of sediment-water exchange and source-sink dynamics of PAHs using fugacity and probabilistic modeling techniques.

2. Materials and methods

2.1 Study areas and sampling

Huixian wetland is the most prominent natural karst wetland located in the Guilin of Guangxi Province, south China. It serves as a globally representative model of karst wetland ecosystems, and plays a critical role as a primary water source for Guilin. Huixian wetland is often referred to as “the kidney of Guilin” owing to its extensive ecological and multifunctional ecosystem services (Xiao et al., 2025). Previous studies have explored the heavy metal accumulation and organochlorine pesticides (OCPs) contamination in both the water and sediment of the wetland (Ba et al., 2022; Xiao et al., 2019). However, limited information was available regarding the transport and transformation of pollutants in the water-sediment system. In this study, field sampling was conducted in the Huixian wetland during the dry and wet seasons, respectively (Fig. 1).

Based on the distinct hydrological characteristics, 29 sampling sites (labeled HW1-1 to

HW1-29) were selected during the dry season to collect water samples (W1-1 to W1-29) and their corresponding surface sediment (SD1-1 to SD1-29). In the wet season, 28 sampling sites (HW2-1 to HW2-29) were designated for the collection of water samples (W2-1 to W2-28) and corresponding sediment samples (SD2-1 to SD2-28). All water samples were stored in pre-cleaned lightproof amber glass bottles (2 L) and kept at -4 °C until analysis. For sediment sampling, a stainless-steel grab sampler was used to collect three samples (0-10cm) at each sampling point. All sediment samples were immediately wrapped in aluminum foil and sealed in clean polyethylene bags for preservation.

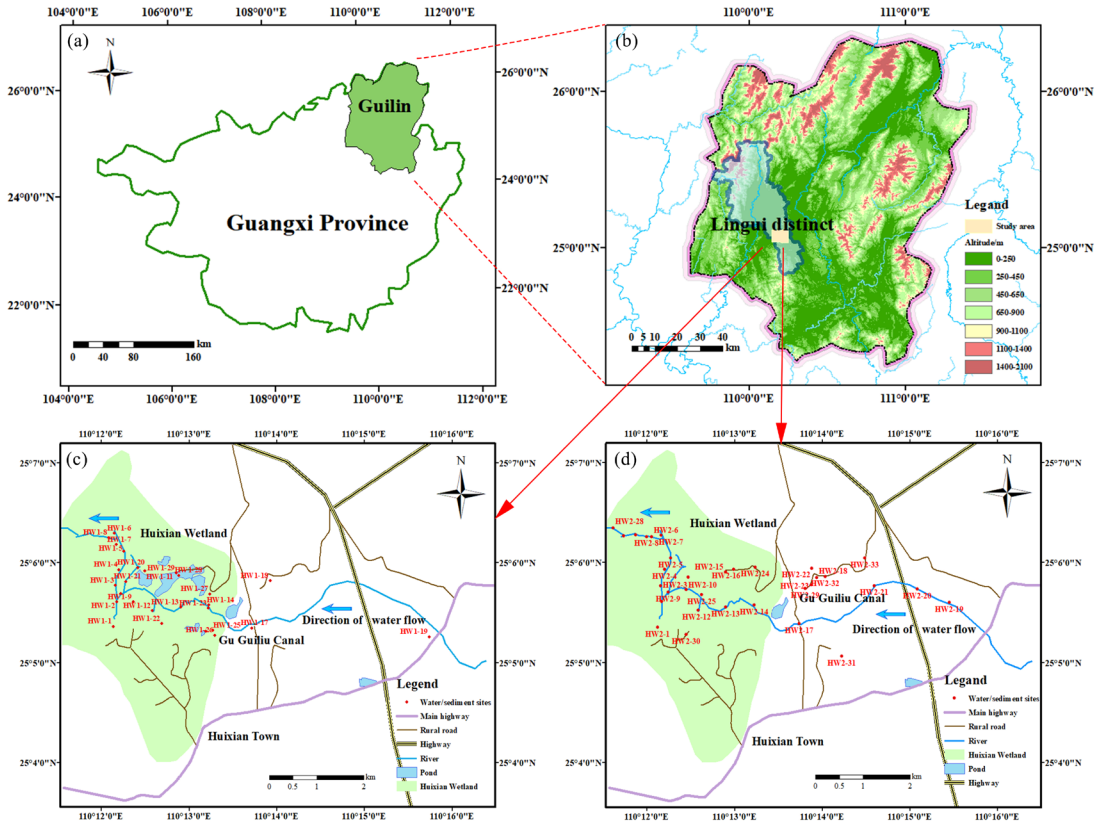

Fig. 1 Research area map, (a): Guangxi Province; (b): Guilin City; (c): Location of sampling sites in the dry season; (d): Location of sampling sites in the wet season

2.2 Chemical analysis

The analytical procedures for PAHs in water and sediment have been reported in previous studies (Hu et al., 2021; Xing et al., 2020). Briefly, sediment and water samples were extracted through a Soxhlet extractor and liquid-liquid extraction. Both extracts were purified on a gel column padded with alumina/silica. Subsequently, the rotary evaporator (Heidolph 4000, Germany) was utilized for evaporation and concentration, reducing the extract to 0.2 mL under a gentle nitrogen stream (purity ≥ 99.999%). Prior to instrumental analysis (GC-MS, Agilent 6890N-5975MSD, equipped with a DB-5MS capillary column, America), a known quantity of hexamethylbenzene (HMB) with 1000ng (Dr. Ehrensorfer, Germany) was added to the final eluate as an internal standard. Detailed sample extraction, purification procedures, and chromatographic conditions are described in Text S1 and Table S2. Sediment organic carbon (OC) and total nitrogen (TN) were measured by the vario TOC cube analyzer (Elementar, Germany) (Xing et al., 2023). Meanwhile, OC was characterized by labile OC (LOC) and residual OC (ROC) based on pyrolytic temperature and carbon dioxide content (Hare et al., 2014).

2.3 Quality assurance and control

Quality assurance and quality control measures were strictly carried out in all sample pre-processing. These included parallel samples, process blanks, method blanks, and surrogates. A parallel and a blank sample were added to each batch to detect losses during the experiment. The average recovery of surrogates including Nap-d_8, Ace-d_{10}, Phe-d_{10}, Chr-d_{12} and Pery-d_{12} in all samples were 71.00±8.93%, 83.66±10.52%, 107.16±12.10%, 101.55±14.37% and

91.36±20.86%, respectively. The target can be detected in the blank sample. However, the concentration was far lower than the sample content, and the relative deviation of parallel samples is within effective limits (< ±5%).

2.4 Data processing and statistical analyses

2.4.1 Source apportionment of PAHs

A positive matrix factorization (PMF) model was used for source identification of PAHs which is a multivariate factor analysis tool that decomposes a matrix of speciated sample data into two matrices: factor contributions (G) and factor profiles (F). Bootstrap was applied to estimate the stability of the results by selecting different factors (2-6) to find the optimal number of sources with a random seed in 20 iterations in each run. The analytical residuals of the selected chemical species were mainly distributed in the range of -3 to 3, which indicated that the modeling was representative. The selected results were evaluated by running different Fpeak strength (±05、±1、1.5) to assess the stability of the operating results of the selected source factors. For observed /predicted scatter plot section from the PMF model, the correlation was high between observed and predicted seeing that R^2 of the selected species was >0.9. More information was presented in Text S2.

2.4.2 Fugacity fraction calculation

Fugacity aims to quantify the chemical potential or partial pressure of a chemical substance between media (Zhang et al., 2021), and it has been widely applied to the study of multi-medium diffusion equilibrium. The fugacity formula used in this study is as follows:

$$f_s = \frac{C_s \rho_s}{Z_s} = \frac{C_s \rho_s \cdot H}{K_{OC} \cdot f_{OC}} \quad (2\text{-}1)$$

$$f_w = \frac{C_w}{Z_w} = \frac{10^6 C_W \cdot H}{P_{\text{mol}}} \quad (2\text{-}2)$$

$$\text{ff}_{\text{sw}} = \frac{f_S}{f_S + f_w} = \frac{f_S/f_w}{f_S/f_w + 1} \quad (2\text{-}3)$$

where, ff_{sw} is the fugacity fraction, f_s and f_w (Pa) are the fugacity of PAHs in sediment and water, respectively; C_W and C_S are PAH concentration in water ($ng \cdot L^{-1}$), sediment ($ng \cdot g^{-1}$), respectively; H is the Henry's law constant ($Pa \cdot m^3 \cdot mol^{-1}$); f_{OC} is the organic carbon content ($g \cdot g^{-1}$).

The organic carbon normalized partition coefficient (K_{oc}) is extensively used to analyze the partitioning behavior of PAHs between water and sediment. The equilibrium partitioning coefficient (K_{oc}) determines the sediment-water partitioning degree (Kong et al., 2023). It can be predicted by using the n-octanol/water partition coefficient (K_{ow}) as follows (Chen et al., 2007) :

$$logK_{OC} = 1.0823 logK_{OW} + 0.2447 \quad (2\text{-}4)$$

where K_{oc} is the organic carbon adsorption equilibrium coefficient, and K_{ow} is the octanol-water partition coefficient (Ha et al., 2019).

Importantly, when $ff_{sw} = 0.5$ it represents sediment-water equilibrium; in other words, the net diffusion flux is zero; thus, $ff_{sw} > 0.7$ indicates net migration from sediment to water. Values of $ff_{sw} < 0.3$ represent net deposition to sediment, which can be explained by the fact that the sediment acts as a sink for the PAHs. Due to occasional calculational uncertainties of ff_{sw}, values of the ff_{sw} between 0.30 and 0.70 are treated as water-sediment equilibrium (Hong et al., 2016; Zhao et al., 2021).

2.4.3 Cosine theta similarity metric (*cos θ*)

The cosine theta similarity metric *(cos θ)* is widely used to assess the degree of similarity of PAH congener profiles between two media. The angle cosine between two multivariate vectors was calculated, in this case, the two 1 × 16 matrixes formed by the 16 PAH congeners. The *cos θ* is derived from the product of the Euclidean magnitudes of the two vectors, as follows:

$$\cos\theta = \frac{\sum_{k=1}^{n} (x_k \cdot s_k)}{\sqrt{\sum_{k=1}^{n} {x_k}^2}\sqrt{\sum_{k=1}^{n} {s_k}^2}} \quad (2\text{-}5)$$

where x_k and s_k are the concentration of congener k in one of water, or sediment samples, n is the number PAH congeners analyzed.

2.4.4 Data statistics and analysis

In this study, the linear mixed effect model, Bayesian Gaussian regression model, and Bayesian network model was undertaken using R studio 2024 (Posit, USA) (R package “lme4”, “brms”, and “bayesplot”). Bayesian Gaussian regression and Bayesian network models can reveal causal relationships and probabilistic structures among variables, making them well-suited for handling highly uncertain, multi-source data in environmental systems (Lin et al., 2025; Shihab, 2008). The former was performed to validate the results of the linear mixed effects model. Posterior distributions and 95% credible intervals were employed to assess the uncertainty of the Bayesian network model. Different modeling frameworks were used to examine the robustness and accuracy of the model construction by Log-likelihood (-1230.6), BIC (954.3), accuracy (89.4%). PAHs and LOC were classified into three categories (low, medium, and high concentrations) based on their distribution probabilities. Other statistical analyses were performed using Origin Pro 2024 (OriginLab Corp., USA).

3. Results and discussion

3.1 PAHs occurrence and distribution

3.1.1 Water

As shown in Table S1 and FigS1, the concentrations of the Σ_{16}PAHs in water ranged from 48.29 to 425.05 ng·L^{-1} in dry seasons and 10.01 to 856.39 ng·L^{-1} in wet seasons (coefficient variations: 0.167 -1.468 in dry seasons and 0.191 - 16.359 in wet seasons), with mean values of 181.82 ± 70.88 ng·L^{-1} in the dry season and 164.44 ± 163.55 ng·L^{-1} in the wet season. A significant spatial heterogeneity of PAHs levels was observed, particularly in wet season. Nap and Phe were the two main species of Σ_{16}PAHs in water during both two seasons. Nap accounted for 21.48% and 34.90% of Σ_{16}PAHs in the dry and wet seasons, respectively, while Phe contributed 34.57% and 31.31%. PAHs levels in the dry season were higher than in the wet season. This pattern may be attributed to the effects of wet deposition, where rainfall contributed to the dilution of PAHs and transported PAHs into the karst system (Qi et al., 2023). During the dry season, intensified anthropogenic activities, such as wood and coal burning, contributed additional PAHs that accumulated alongside those transported during the wet season. These combined effects resulted in elevated PAHs concentrations in Huixian Wetland waters (Wu et al., 2021), suggesting that anthropogenic inputs exceeded the natural 'self-purification' capacity of the environment (Semenov et al., 2019).

A similar pattern was presented in both wet and dry seasons, with PAHs distributed in the order: 3-ring > 2-ring > 4-ring > 5-ring > 6-ring. Meanwhile, the significant difference of 4-rings ($p < 0.001$), 6-rings ($p < 0.01$), 2-rings and 5-rings ($p<0.05$) between wet and dry seasons

was observed in Fig 2, which attributed to the differences in emission sources and environmental factors. This implies that 3-ring PAHs have always played a dominant role in aquatic environments. Compared to other wetlands, the PAHs levels of overlying water in the Huixian wetland were higher than the previously reported concentraions, such as, Anzali wetland, Iran (5.14 - 253.37 $ng \cdot L^{-1}$) (Yuan et al., 2014), a karst spring systems from Western Hubei, China (4.56 - 11.4 $ng \cdot L^{-1}$) (Chen et al., 2022). These findings indicate that the occurrence of higher PAHs in Huixian wetlands in karst systems probably occurred due to the thinner soil layer and more developed fissures, which facilitated the rapid infiltration and accumulation of pollutants in water environment.

3.1.2 Sediment

Phe was the most abundant species in sediment, accounting for 14.47% and 11.27% of $\sum_{16}$PAHs in the dry and wet seasons, respectively. Distinct temporal variations of PAHs concentrations in sediment were more evident, such as the higher spatial variation of $\sum_{16}$PAHs in sediment (coefficient variations: 0.100 ~ 36.638 in wet seasons and 0.126 ~ 41.177 in dry seasons). Contrary to the results from water, PAHs levels in sediment of dry seasons presented higher spatial heterogeneity, implying a distinct environmental fate of PAHs at sediment-water interface driven by seasonal transitions. $\sum_{16}$PAHs percentage was in the order of 4-ring PAHs (33.58%) > 3-ring PAHs (23.81%) > 5-ring PAHs (21.13%) > 6-ring PAHs (19.99%) > 2-ring PAHs (1.50%) in the dry season. As for the wet season, the distribution was 4-ring PAHs (39.78%) > 5-ring PAHs (22.13%) > 3-ring PAHs (19.93%) > 6-ring PAHs (16.63%) > 2-ring PAHs (1.55%). It is worth noting that medium molecular weight (MMW, 3-rings and 4-rings)

PAHs and high molecular weight (HMW, 5-rings and 6-rings) PAHs were predominant in sediment. Their dominance may be attributed to their specific physicochemical properties, including lower water solubility, greater hydrophobicity, and higher partition coefficients compared to low molecular weight (LMW) PAHs (PAUZI, 2006). These results were consistent with previous findings in Laolongdong underground river system (Lan et al., 2016) and the Guozhuang karst groundwater system (Shao et al., 2014), where the lower vapor pressure and water solubility of HMW-PAHs contributed to their accumulation in sediments.

Generally, PAH concentrations in the Huixian Wetland were much higher than those previously reported for many other wetlands, including the Ashtamudi wetland from southwest coast, India (158.23 - 202.81 $ng \cdot g^{-1}$) (Li et al., 2015; Sreedevi and Harikumar, 2023), wetland habitats in Northern Adriatic, Italy (310 - 1550 $ng \cdot g^{-1}$) (Guerra, 2012), Anzali Wetland, Iran (212 - 2674 $ng \cdot g^{-1}$) (Yuan et al., 2014), the Wang Lake wetland, China (13.8 - 568 $ng \cdot g^{-1}$) (Shi et al., 2022), the Dajiuhu Sub-alpine Wetland, China (7.30 - 191.48 $ng \cdot g^{-1}$) (Xing et al., 2020). Additionally, PAH concentrations increased from the wet to dry season at 72.4% of sediment sampling sites, whereas 62.06% of overlying water sites showed a decrease. The seasonal differences suggested complex secondary release processes and accumulation of PAHs in Huixian wetlands, which may be influenced by seasonal hydrological conditions and intensified anthropogenic inputs.

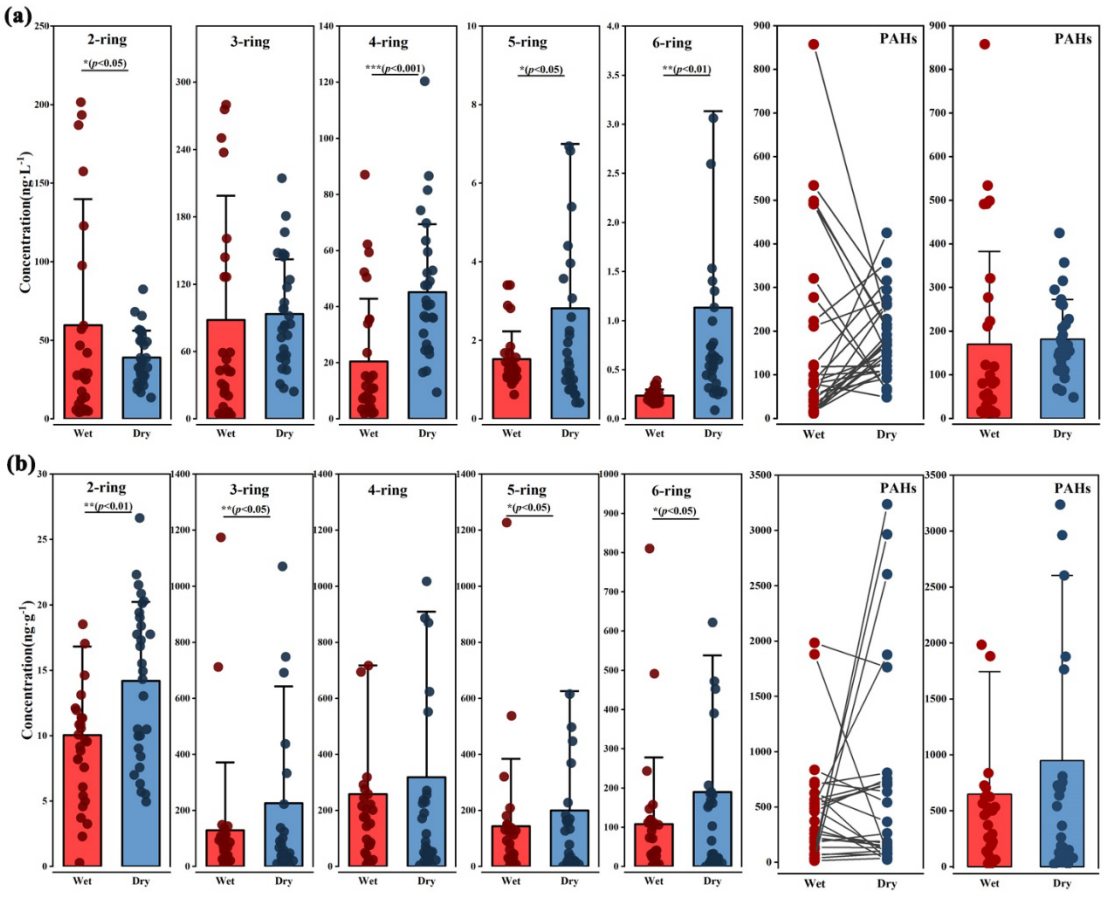

Fig. 2 The PAHs levels at different sites between wet and dry seasons in water (a) and in sediment (b).

3.2 Variations in source identification

PMF models have previously been performed to identify potential sources of PAHs. Previous studies have shown that PAHs sources in overlying water differ significantly from those in sediments (Hu et al., 2022; Liu et al., 2023). As a result, total concentrations of PAHs (TPAHs) of multiphase media (air + particle for atmosphere samples; water + sediment for lake samples) should be used since their levels may change due to the environmental fate of these compounds (such as phase transport and secondary release) (Tobiszewski and Namiesnik, 2012). In this study, the concentration of PAHs in sediment (SPAHs) and multiphase media (water + sediment) were employed separately to investigate their potential sources, with an

optimal four-factor solution was provided with a minimum Q value. As shown in Fig S2, the main loadings representing each factor remained consistent for both SPAHs and TPAHs across wet and dry seasons. In brief, F1 exhibited high loading of Nap (>60%), which is usually regarded as indicators of petroleum-related products (Li et al., 2024b). F2 was characterized by the BaA, Chr, BbF, BkF, BaP, IcdP, DahA, and BghiP. Generally, Chr, BbF, and BkF were associated with the diesel-powered vehicles and BaP, DahA, IcdP, and BghiP could be represented the gasoline-powered vehicles emissions (Ashayeri et al., 2018; Harrison et al., 1996). Therefore, F2 was labeled as vehicles emissions. F3 exhibited the high loading of Acy, Ace, and Flu, wherein Flu and Ace were regarded as typical indicators of biomass-burning sources (Deng et al., 2024; Ma et al., 2020). F4 was heavily weighted by Phe, Ant, Fla, and Pyr. Phe, Fla and Pyr are good indicators of coal combustion, as suggested by previous research (Zhang et al., 2024).

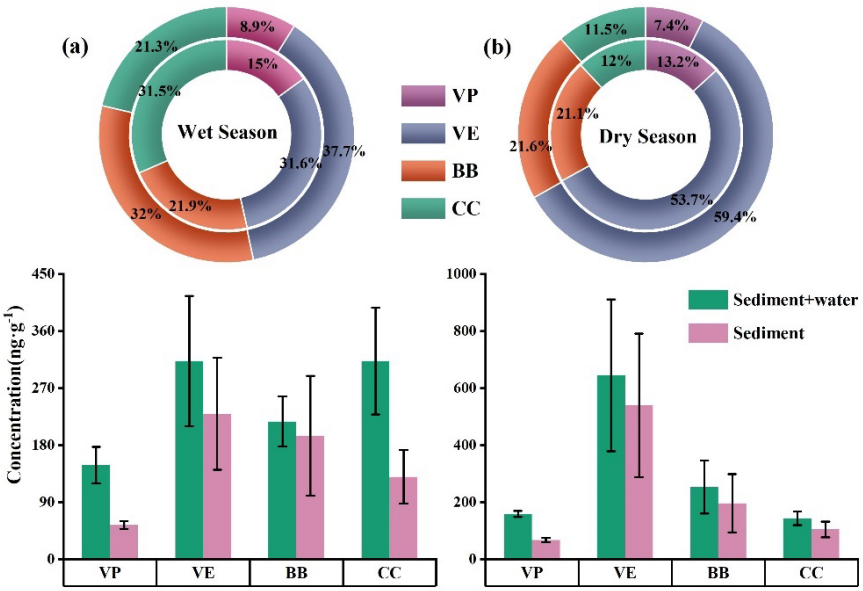

Fig.3. Results of the PMF model: Source profiles of four factor based on TPAHs and SPAHs in wet (a) and dry seasons (b).

Using the results of the PMF model the concentration and percentage of the four source types across wet and dry seasons are shown in Fig 3. The primary source of PAHs was attributed to vehicles emissions (VE) between wet and dry seasons agreeing with previous study (Deng et al., 2024). The source contributions from volatilization of petroleum and related products (VP) and coal combustion (CC) presented significant difference (greater than 50%) from SPAHs to TPAHs in wet seasons, revealing that these PAH originating from VP and CC were mainly influenced by transport at the sediment-water interface. However, the contribution of CC could be underestimated if only SPAHs was used for source identification, which could potentially lead to the inappropriate management measures. Similar patterns of PAH originating from VP were also presented in dry seasons. There were varying degrees of difference (greater than 10%) in VE and biomass burning (BB) between SPAHs and TPAHs. VE showed a maximum increase from wet to dry seasons, which could be attributed to more stable flow rates and higher atmospheric deposition during the dry season (Jiang et al., 2018; Xu et al., 2019). The decrease of CC could be caused by the reduction of industrial coal-fired emissions from wet to dry seasons (Ore et al., 2023). In summary, the transport process of PAHs in multiphase media should be combined with source apportionment. Identifying potential sources through TPAHs could be more accurate for the development and implementation of pollution control measures.

3.3 Sediment-water exchange

The potential for transport (and direction) of PAHs between sediment and overlying water

are influenced by sources of emission and the effect of the physicochemical properties of sediment and water, particularly under considerable seasonal variation. For this study the cosine theta similarity metric *(cos θ)* was used to capture the similarity of PAHs profile between water and sediment (Shi et al., 2022). Generally, higher *cos θ* value (approaching 1) demonstrate substantial similarity. As shown in Fig S3, the similarity of PAHs between water and sediment in dry seasons was clear, with 34.48% of sample sites exhibiting higher cos θ values (exceeding 0.80). In contrast, a reduced similarity of PAHs levels was present in wet seasons, suggesting that transport potential of sediment to overlying water in the dry seasons was greater than in the wet seasons.

The fugacity fraction (ff_{sw}) between water and sediment was calculated through the fugacity model theory to further understand the behavior and fate of PAHs, with the results presented in Fig 4. ff_{sw} values of most PAHs in wet seasons ranged from 0.3 to 0.7, revealing the equilibrium between sediments and overlying water. Regarding the HMW-PAHs in dry seasons, most of the ff_{sw} was below 0.3, showing the unsaturated condition for sediment and net transport from the water to the sediment. This may be attributed to their hydrophobic properties since HMW-PAHs are more strongly adsorbed in sediment (Wang et al., 2011). In general, the ff_{sw} values presented a gradual decline in average value with increasing molecular weight of PAHs, similar to previously published results (Liu et al., 2021). However, the ff_{sw} of PAHs in current study was slightly higher than for other areas, e.g. Yangtze River Delta, China(Liu et al., 2021), Taige Canal, China(Kong et al., 2023), Dajiuhu subalpine wetland, China(Hu et al., 2022). A potential reason for this is that the soluble carbonate rocks in karst areas have poor

329 ability of blocking and purifying pollutants (Zhou et al., 2023).

330 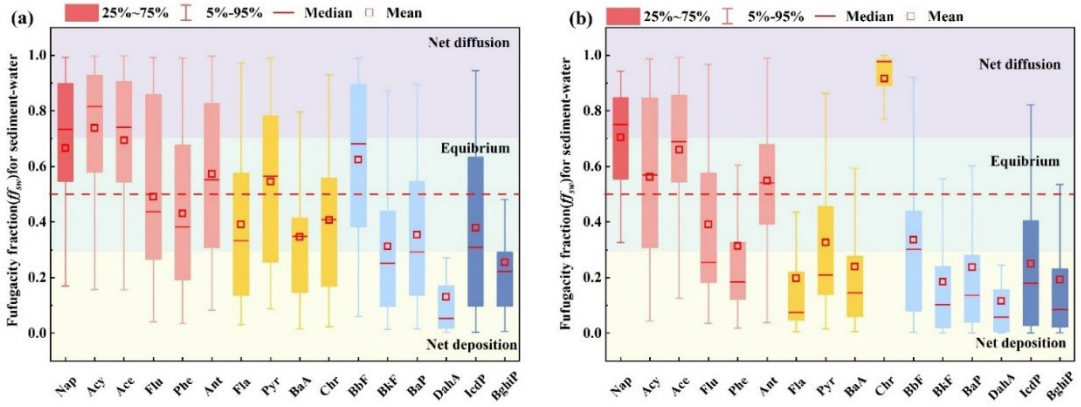

331 Fig.4. Fugacity fraction of PAHs between sediment and water (ff_{sw}) in wet(a) and dry seasons(b).

332 Results from this study showed that sediment contained more PAHs in dry seasons than in
333 wet seasons. Closer hydrological connectivity between sediment and overlying water is usually
334 prevalent in wet seasons (Chen et al., 2023; Jiang et al., 2018; Zhang et al., 2021). Consequently,
335 it was assumed that PAHs in sediment and water systems in wet seasons tend towards
336 equilibrium. We explored the relationship between different WPAHs/TPAHs and their LogKow
337 and calculated the gap (as shown in Fig 5, area of shaded part) between the two fitting curves
338 for wet and dry seasons to expressing the re-release potential of PAHs. The result suggested
339 that the sediment PAHs which accumulate in dry seasons could be considered as secondary
340 emission source. Meanwhile, the difference of secondary release potential between wet and dry
341 seasons (ΔWPAHs/TPAHs) was strongly dependent on the physicochemical properties of PAHs
342 in Fig S4. PAHs with 3-rings and 4-rings PAHs (4<Log Kow<6) showed a higher secondary
343 release potential. Similar to these findings, previous studies have also reported that LMW-PAHs
344 tend to migrate from surface water to sediment, and yet the observed release from porewater to
345 overlying water provided a greater input of 3-rings and 4-rings PAHs at the sediment-water

interface (Moran et al., 2024). Potential reasons were the stronger interaction between dissolved organic matter (humic acid-like substances) and 3-rings and 4-rings PAHs (Phe, Fla, Chr, and BkF) (Sun et al., 2023). Above all, these results reinforce the need to include seasonality when assessing re-release potential of PAHs across the sediment-water interface.

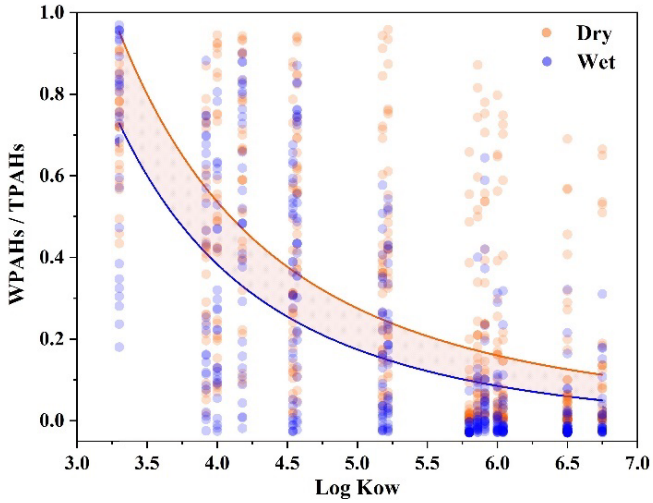

Fig.5. Re-release potential of 16PAHs in the Huixian wetland in wet and dry seasons.

3.4 Understanding for the source-sink processes of PAHs

As discussed above, a significant difference in the re-release potential of PAHs between wet and dry seasons was observed. However, sediment physicochemical properties were equally important to determine the dominant factors of PAHs transport in sediment-water interface beyond the physicochemical characteristics of PAHs (Xu et al., 2020). A linear mixed effect model was employed to identify the key driver of PAH accumulation in sediment and to estimate both the fixed effects (FE) and random effects (RE) of PAHs transport in sediment-water interface (Xie et al., 2023). Specifically, fixed effects often express the correlation of pollutant and explaining variable, while random effects account for variability of pollutants and

362 sites (such as pollutant source emissions) (Buscemi and Plaia, 2020). Results showed that
363 season effects and LOC played a significant role in PAH transport in Fig 6. LOC was more
364 easily influenced by the attachment to suspended particles, which facilitated the adsorption and
365 transport of PAHs at the sediment-water interface. LOC is more effective for the multi-media
366 transport of LWM-PAHs (Liu et al., 2025a). Meanwhile, a higher contribution of ROC for
367 HWM-PAHs sorption was evident compared to LWM-PAHs, which was attributed to more
368 adsorption sites and higher bond energy between HWM-PAHs and ROC (Cui et al., 2025; Yu
369 et al., 2024). The effect of seasonal variation on LWM-PAHs was significantly higher than that
370 for HWM-PAHs. Both physicochemical parameters of PAHs compounds and environmental
371 factors (temperature, hydrodynamics, and rainfall) made a notable variation in the extent of
372 influence on the transport of PAHs, meaning that LWM-PAHs were more labile than HWM-
373 PAHs (Huang et al., 2019).

374 Additionally, the interaction effect (IE) of season and LOC was also quantified in this
375 study, in which IE served as the important part of FE (Fig 6c). The contribution of IE for PAHs
376 with 2 rings to 6 rings was similar to the result for the sediment-water exchange patterns
377 observed in Fig 6. 3 rings and 4 rings PAHs presented higher interaction potential at the
378 sediment- water interface. The potential mechanism underlying the association between
379 molecular weight difference and multi-media transport of PAHs was sorption to the labile
380 fraction of organic matter. Specifically, the LOC fraction often includes the humic acid (HA)
381 and fulvic acid (FA). The availability of 3 ring and 4 ring PAHs were strongly correlated with
382 HA and FA owing to their strong affinity (Ukalska-Jaruga and Smreczak, 2020). As a result, the

seasonal fluctuations of LOC determined the higher secondary release potential of PAHs at the sediment-water interface.

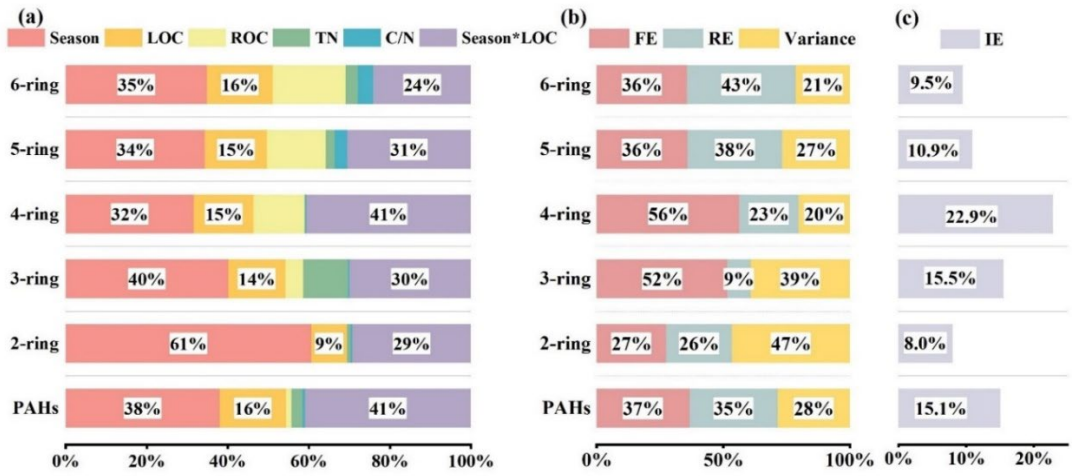

Fig.6. The percentage of physicochemical parameters of sediment (a), fixed effects, random effects, variance (b), and interaction effects (c) based on the linear mixed effect model.

A more detailed investigation into the source-sink process of PAHs at the sediment -water interface was conducted using a Bayesian network model. Firstly, a Bayesian Gaussian regression model was applied to validate the results of the linear mixed effect model in Fig S5. A significant negative effect of wet seasons on PAHs occurrence (estimate= -1371.36, 95% confidence interval [-2494.97, -287.13]) revealed the potential transport of PAHs from water to sediment during high-flow conditions. This could be attributed to the changes of hydrodynamic conditions as PAHs may be diluted by enhanced runoff and water exchange (Yuan et al., 2015). Meanwhile, a significant positive interaction between seasons and LOC (estimate= 336.55, 95% confidence interval [44.60, 649.30]) revealed a synergistic effect influencing the migration of PAHs. The conditional effect of seasons and LOC (in Fig S6) further suggested that the dynamic

399 changes in sediment LOC may enhance the release of PAHs during dry seasons. Additionally,
400 a robust probabilistic framework was provided to capture the heterogeneous interactions
401 between PAHs and environmental factors, as illustrated in Fig S7. The Bayesian network model
402 results indicated that lower PAH concentrations were observed in the overlying water in Fig 7,
403 while PAHs in sediment were dominated by high concentrations in wet seasons, revealing a
404 significant “sink” effect of sediment on PAHs. In contrast, concentrations of PAHs in water
405 increased and the proportion of high PAHs levels in sediment decreased during dry seasons.
406 There was, therefore, a release process of PAHs from sediment to overlying water, with
407 sediment becoming a potential “secondary source”. Previous studies have also observed the
408 similar pattern using diffusion models, with higher PAH concentrartions accumulating in
409 sediment during rainy seasons with increased PAHs concentration in water during dry seasons
410 (Zhang et al., 2024). Zhang et al. (2021) have also reported that sediment acted as a secondary
411 emission source of PAHs in dry-wet cycle using fugacity calculations, supporting the temporal
412 transfer patterns observed by this study. However, the Bayesian approach allowed for a detailed
413 expression of uncertainty and complex interaction effect between PAHs and environmental
414 factors. Therefore, a deeper insight into the source-sink processes of PAHs was provided by
415 this study. Meanwhile, these seasonal differences suggest that the migration and transport
416 mechanism of PAHs at the sediment-water interface changes under wet and dry seasons, which
417 is of importance for water pollution control.

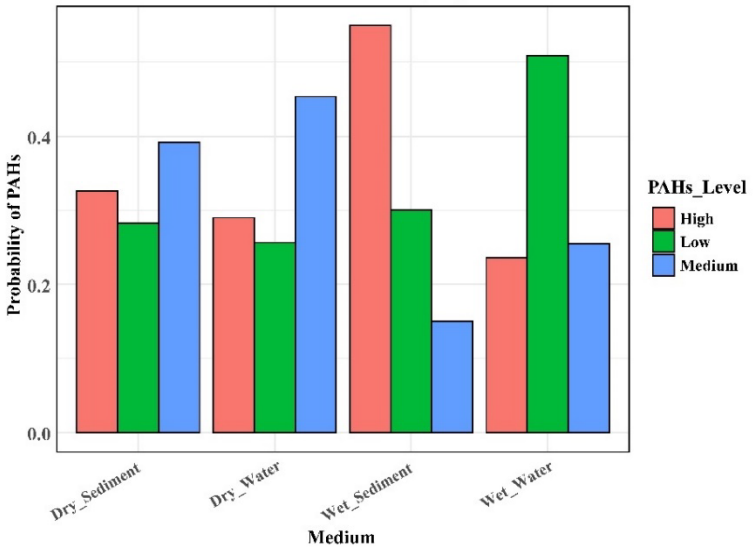

Fig.7. PAHs levels of different medium during dry and wet seasons based on the results of Bayesian network model.

4. Conclusion and environmental significance

PAHs occurrence, source apportionment, sediment-water exchange, and source-sink processes have been studied in detail in a typical karst wetland. The average concentration of PAHs in overlying water were 181.82 ± 70.88 ng·L^{-1} in the dry season and 164.44 ± 163.55 ng·L^{-1} in the wet season. PAH concentrations in sediment exhibited seasonal variation, with an average of 948.86 ± 59.08 ng·g^{-1} in the dry season and 649.88 ± 39.09 ng·g^{-1} in the wet season. Four potential sources of PAHs were identified. However, significant differences in source identification based on TPAHs and SPAHs were presented, implying that the transport dynamics of PAHs in multiphase media should be combined with an assessment of source apportionment. Higher re-release potential of PAHs (3 rings and 4 rings) in dry seasons was captured using a traditional fugacity model aproach. Meanwhile, the results of a linear mixed effect model revealed the contribution of both fixed and random effects. Seasonal effects and LOC were found to play a significant role in PAHs transport. Similarly, the interaction effect of

3 rings and 4 ringed PAHs presented a higher contribution to variability. A Bayesian network model was used to predict the source-sink exchange for PAHs. A significant “sink” effect of sediment on PAHs was captured in wet seasons, yet sediment became a potential “secondary source” in dry seasons.

This study provides novel insights into how seasonal variations, carbon fractions (e.g., LOC and ROC), and multiphase transport processes influence the redistribution of PAHs between sediment and overlying water. By integrating Bayesian modeling approaches, the findings help quantify secondary release dynamics and source- sink transformation processes. Seasonal effects and LOC played a significant role in PAHs transport across sediment- water interface. These results are essential for improving risk assessment frameworks and supporting effective management of organic pollutants in karst environments, and inform targeted pollution control strategies.

Acknowledgement

The research was supported by the National Key Research and Development Program of China (2023YFC3709803); the National Natural Science Foundation of China (No. 42377235); the Fundamental Research Funds for the Central Universities, China University of Geosciences (Wuhan) (No. G1323523063; No. G1323524009); Weijie Liu acknowledges financial supports from the China Scholarship Council (No.202406410108).

Author contributions statement

Weijie Liu: Conceptualization; Data curation; Formal analysis; Investigation; Methodology; Software; Supervision; Visualization; Writing – original draft; Writing – review & editing; **Xinli Xing:** Conceptualization; Formal analysis; Investigation; Project administration; Data Curation; Writing - Review & Editing; Supervision; **Xin Li:** Formal analysis; Methodology; Investigation; Visualization; Writing – original draft; **Cheng Cheng:** Formal analysis; Investigation; Data Curation; **Mingming Shi:** Formal analysis; Methodology; Investigation; **Tianpeng Hu:** Formal analysis; Methodology; Investigation; **Yuan Zhang:** Formal analysis; Investigation; **Andrew Sweetman:** Conceptualization; Formal analysis; Writing - Review & Editing; **Shihua Qi:** Data curation; Supervision; Project administration;

References

Ashayeri NY, Keshavarzi B, Moore F, Kersten M, Yazdi M, Lahijanzadeh AR. Presence of polycyclic aromatic hydrocarbons in sediments and surface water from Shadegan wetland - Iran: A focus on source apportionment, human and ecological risk assessment and Sediment-Water Exchange. Ecotoxicology and Environmental Safety 2018; 148: 1054-1066.http://doi.org/10.1016/j.ecoenv.2017.11.055.

Ba JJ, Gao FF, Peng C, Li J. Characteristics of nitrate and heavy metals pollution in Huixian Wetland and its health risk assessment. Alexandria Engineering Journal 2022; 61.http://doi.org/10.1016/j.aej.2022.02.045.

Buscemi S, Plaia A. Model selection in linear mixed-effect models. Asta-Advances in Statistical Analysis 2020; 104: 529-575.http://doi.org/10.1007/s10182-019-00359-z.

Chen CT, Lin T, Sun X, Wu ZL, Tang JH. Spatiotemporal distribution and particle-water partitioning of polycyclic aromatic hydrocarbons in Bohai Sea, China. Water Research 2023; 244.http://doi.org/10.1016/j.watres.2023.120440.

Chen W, Zhang ZQ, Zhu Y, Wang XZ, Wang LL, Xiong JW, et al. Distribution, sources and transport of polycyclic aromatic hydrocarbons (PAHs) in karst spring systems from Western Hubei, Central China. Chemosphere 2022; 300.http://doi.org/10.1016/j.chemosphere.2022.134502.

Chen YY, Zhu LZ, Zhou RB. Characterization and distribution of polycyclic aromatic hydrocarbon in surface water and sediment from Qiantang River, China. Journal of Hazardous Materials 2007; 141: 148-155.http://doi.org/10.1016/j.jhazmat.2006.06.106.

Cheng C, Hu TP, Liu WJ, Mao Y, Shi MM, Xu A, et al. Modern lake sedimentary record of PAHs and OCPs in a typical karst wetland, south China: Response to human activities and environmental changes. Environmental Pollution 2021; 291.http://doi.org/10.1016/j.envpol.2021.118173.

Cui MH, Zhang J, Huang CH, Xu SY, Czech B, Han JG, et al. The role of nano-biochar reduces the impact of phenanthrene on wheat photosynthesis. Environmental Science-Nano 2025; 12: 1881-1895.http://doi.org/10.1039/d4en00887a.

Deng XQ, Mao LJ, Peng M, Cai YQ, Wang T, Luo ZH, et al. Polycyclic aromatic hydrocarbons in coastal rivers in Jiangsu Province, China: Spatial distribution, source apportionment

and human impacts. Journal of Hazardous Materials 2024; 466.http://doi.org/10.1016/j.jhazmat.2024.133576.

Dippong T, Senila M, Cadar O, Resz MA. Assessment of the heavy metal pollution degree and potential health risk implications in lakes and fish from northern Romania. Journal of Environmental Chemical Engineering 2024; 12.http://doi.org/10.1016/j.jece.2024.112217.

Gong XH, Zhao ZH, Zhang L, Yao SC, Xue B. North-south geographic heterogeneity and control strategies for polycyclic aromatic hydrocarbons (PAHs) in Chinese lake sediments illustrated by forward and backward source apportionments. Journal of Hazardous Materials 2022; 431.http://doi.org/10.1016/j.jhazmat.2022.128545.

Guerra R. Polycyclic Aromatic Hydrocarbons, Polychlorinated Biphenyls and Trace Metals in Sediments from a Coastal Lagoon (Northern Adriatic, Italy). Water Air and Soil Pollution 2012; 223: 85-98.http://doi.org/10.1007/s11270-011-0841-6.

Guo JX, Fang J, Cao JJ. Characteristics of petroleum contaminants and their distribution in Lake Taihu, China. Chemistry Central Journal 2012; 6.http://doi.org/10.1186/1752-153x-6-92.

Ha H, Park K, Kang G, Lee S. QSAR study using acute toxicity of Daphnia magna and Hyalella azteca through exposure to polycyclic aromatic hydrocarbons (PAHs). ECOTOXICOLOGY 2019; 28: 333-342.http://doi.org/10.1007/s10646-019-02025-1.

514 Han DM, Currell MJ. Persistent organic pollutants in China's surface water systems. Science
515 of the Total Environment 2017; 580: 602-
516 625.http://doi.org/10.1016/j.scitotenv.2016.12.007.
517 Hare AA, Kuzyk ZZA, Macdonald RW, Sanei H, Barber D, Stern GA, et al. Characterization
518 of sedimentary organic matter in recent marine sediments from Hudson Bay, Canada,
519 by Rock-Eval pyrolysis. Organic Geochemistry 2014; 68: 52-
520 60.http://doi.org/10.1016/j.orggeochem.2014.01.007.
521 Harrison RM, Smith DJT, Luhana L. Source apportionment of atmospheric polycyclic aromatic
522 hydrocarbons collected from an urban location in Birmingham, UK. Environmental
523 Science & Technology 1996; 30: 825-832.http://doi.org/10.1021/es950252d.
524 He Y, Yang C, He W, Xu FL. Nationwide health risk assessment of juvenile exposure to
525 polycyclic aromatic hydrocarbons (PAHs) in the water body of Chinese lakes. Science
526 of the Total Environment 2020; 723.http://doi.org/10.1016/j.scitotenv.2020.138099.
527 Hong WJ, Jia HL, Li YF, Sun YQ, Liu XJ, Wang L. Polycyclic aromatic hydrocarbons (PAHs)
528 and alkylated PAHs in the coastal seawater, surface sediment and oyster from Dalian,
529 Northeast China. Ecotoxicology and Environmental Safety 2016; 128: 11-
530 20.http://doi.org/10.1016/j.ecoenv.2016.02.003.
531 Hu TP, Mao Y, Ke YP, Liu WJ, Cheng C, Shi MM, et al. Spatial and seasonal variations of
532 PAHs in soil, air, and atmospheric bulk deposition along the plain to mountain transect
533 in Hubei province, central China: Air-soil exchange and long-range atmospheric

transport. Environmental Pollution 2021; 291.http://doi.org/10.1016/j.envpol.2021.118139.

Hu TP, Shi MM, Mao Y, Liu WJ, Li M, Yu Y, et al. The characteristics of polycyclic aromatic hydrocarbons and heavy metals in water and sediment of dajiuhu subalpine wetland, shennongjia, central China, 2018-2020: Insights for sources, sediment-water exchange, and ecological risk. Chemosphere 2022; 309.http://doi.org/10.1016/j.chemosphere.2022.136788.

Huang YP, Sun X, Liu M, Zhu JM, Yang J, Du WN, et al. A multimedia fugacity model to estimate the fate and transport of polycyclic aromatic hydrocarbons (PAHs) in a largely urbanized area, Shanghai, China. Chemosphere 2019; 217: 298-307.http://doi.org/10.1016/j.chemosphere.2018.10.172.

Jiang L, Ma XD, Wang YW, Gao W, Liao CY, Gong YF, et al. Land-Ocean Exchange Mechanism of Chlorinated Paraffins and Polycyclic Aromatic Hydrocarbons with Diverse Sources in a Coastal Zone Boundary Area, North China: The Role of Regional Atmospheric Transmission. Environmental Science & Technology 2022; 56: 12852-12862.http://doi.org/10.1021/acs.est.2c00742.

Jiang YQ, Lin T, Wu ZL, Li YY, Li ZX, Guo ZG, et al. Seasonal atmospheric deposition and air-sea gas exchange of polycyclic aromatic hydrocarbons over the Yangtze River Estuary, East China Sea: Implications for source-sink processes. Atmospheric Environment 2018; 178: 31-40.http://doi.org/10.1016/j.atmosenv.2018.01.031.

554 Kong JJ, Ma T, Cao XY, Li WD, Zhu FX, He H, et al. Occurrence, partition behavior, source
555 and ecological risk assessment of nitro-PAHs in the sediment and water of Taige Canal,
556 China. Journal of Environmental Sciences 2023; 124: 782-
557 793.http://doi.org/10.1016/j.jes.2022.02.034.
558 Lahens L, Correa JA, Cabana H, Huot Y, Segura PA. Influence of anthropogenic activities on
559 the trace organic contamination of lakes. Science of the Total Environment 2024;
560 949.http://doi.org/10.1016/j.scitotenv.2024.175087.
561 Lan JC, Sun YC, Xiao SZ, Yuan DX. Polycyclic aromatic hydrocarbon contamination in a
562 highly vulnerable underground river system in Chongqing, Southwest China. Journal
563 of Geochemical Exploration 2016; 168: 65-
564 71.http://doi.org/10.1016/j.gexplo.2016.05.013.
565 Li DP, Zhu ZJ, Cao XC, Yang TW, An SQ. Ecological risk of polycyclic aromatic hydrocarbons
566 (PAHs) and organochlorine pesticides (OCPs) in the sediment of a protected karst
567 plateau lake (Caohai) wetland in China. Marine Pollution Bulletin 2024a;
568 201.http://doi.org/10.1016/j.marpolbul.2024.116199.
569 Li JF, Dong H, Zhang DH, Han B, Zhu CJ, Liu SP, et al. Sources and ecological risk assessment
570 of PAHs in surface sediments from Bohai Sea and northern part of the Yellow Sea,
571 China. Marine Pollution Bulletin 2015; 96: 485-
572 490.http://doi.org/10.1016/j.marpolbul.2015.05.002.

573 Li RF, Luo Y, Zhu X, Zhang J, Wang ZY, Yang WY, et al. Anthropogenic impacts on polycyclic
574 aromatic hydrocarbons in surface water: Evidence from the COVID-19 lockdown.
575 Water Research 2024b; 262.http://doi.org/10.1016/j.watres.2024.122143.
576 Lin YC, Lin YT, Chen CR, Lai CY. Meteorological and traffic effects on air pollutants using
577 Bayesian networks and deep learning. Journal of Environmental Sciences 2025; 152:
578 54-70.http://doi.org/10.1016/j.jes.2024.01.057.
579 Liu CY, Huang ZF, Qadeer A, Liu Y, Qiao XC, Zheng BH, et al. The sediment-water diffusion
580 and risk assessment of PAHs in different types of drinking water sources in the Yangtze
581 River Delta, China. Journal of Cleaner Production 2021;
582 309.http://doi.org/10.1016/j.jclepro.2021.127456.
583 Liu K, Wang XM, Zhang HB, Wei YW, Zhao G, Liu X, et al. Sources, transport and fate of
584 polycyclic aromatic hydrocarbons (PAHs) in a typical river-estuary system in the North
585 China: From a new perspective of PAHs loading. Marine Pollution Bulletin 2025a;
586 214.http://doi.org/10.1016/j.marpolbul.2025.117692.
587 Liu W, Xing X, Zou Y, Li X, Gao Y, Liu Y, et al. Novel insights into PAHs accumulation and
588 multi-method characterization of interaction between groundwater and surface water
589 in middle Yangtze River: Hydrochemistry, isotope hydrology and fractionation effect.
590 Sci Total Environ 2025b; 958: 178023.http://doi.org/10.1016/j.scitotenv.2024.178023.
591 Liu Y, He Y, Liu Y, Liu HJ, Tao S, Liu WX. Source identification and ecological risks of parent
592 and substituted polycyclic aromatic hydrocarbons in river surface sediment-pore water

593 systems: Effects of multiple factors. Science of the Total Environment 2023;
594 858.http://doi.org/10.1016/j.scitotenv.2022.159921.
595 Lu ZY, Tian WJ, Chen Z, Chu ML, Zhang SR, Liu BK, et al. Release of PAHs from sediments
596 to seawater under wave: Indoor microcosms and level IV fugacity models. Journal of
597 Hazardous Materials 2024; 474.http://doi.org/10.1016/j.jhazmat.2024.134799.
598 Luo J, Huang GB, Wang M, Zhang YN, Liu ZX, Zhang Q, et al. Composition characteristics,
599 source analysis and risk assessment of PAHs in surface waters of Lipu. Journal of
600 Hazardous Materials 2025; 490.http://doi.org/10.1016/j.jhazmat.2025.137733.
601 Ma XH, Wan HB, Zhou J, Luo D, Huang T, Yang H, et al. Sediment record of polycyclic
602 aromatic hydrocarbons in Dianchi lake, southwest China: Influence of energy structure
603 changes and economic development. Chemosphere 2020;
604 248.http://doi.org/10.1016/j.chemosphere.2020.126015.
605 Mackay D. FINDING FUGACITY FEASIBLE. Environmental Science & Technology 1979;
606 13: 1218-1223.
607 Miao XY, Hao YP, Cai JW, Xie YC, Zhang JR. The distribution, sources and health risk of
608 polycyclic aromatic hydrocarbons (PAHs) in sediments of Liujiang River Basin: A field
609 study in typical karstic river. Marine Pollution Bulletin 2023;
610 188.http://doi.org/10.1016/j.marpolbul.2023.114666.
611 Moran IL, Ghetu CC, Scott RP, Tidwell LG, Hoffman PD, Anderson KA. Divergent Transport
612 Dynamics of Alkylated versus Unsubstituted Polycyclic Aromatic Hydrocarbons at the

Air-Water and Sediment-Water Interfaces at a Legacy Creosote Site. Acs Es&T Water 2024; 5: 146-155.http://doi.org/10.1021/acsestwater.4c00737.

Nybom I, van Grimbergen J, Forsell M, Mustajärvi L, Martens J, Sobek A. Water column organic carbon composition as driver for water-sediment fluxes of hazardous pollutants in a coastal environment. Journal of Hazardous Materials 2024; 465.http://doi.org/10.1016/j.jhazmat.2023.133393.

Ore OT, Bayode AA, Badamasi H, Olusola JA, Durodola SS, Akeremale OK, et al. Seasonal distribution, source apportionment and risk assessment of polycyclic aromatic hydrocarbons in groundwaters in Owo, Southwestern Nigeria. Water Practice and Technology 2023; 18: 3365-3376.http://doi.org/10.2166/wpt.2023.217.

PAUZI ZM, AZRIL, M. A. Distribution of Polycyclic Aromatic Hydrocarbon (PAHs) in sediments in the Langat Estuary. Coastal marine science 2006; Vol. 30 No. 1: 387-395.

Qi X, Lan JC, Sun YC, Wang SS, Liu L, Wang JX, et al. Linking PAHs concentration, risk to PAHs source shift in soil and water in epikarst spring systems, Southwest China. Ecotoxicology and Environmental Safety 2023; 264.http://doi.org/10.1016/j.ecoenv.2023.115465.

Semenov MY, Semenov YM, Silaev AV, Begunova LA. Assessing the Self-Purification Capacity of Surface Waters in Lake Baikal Watershed. Water 2019; 11.http://doi.org/10.3390/w11071505.

632 Shao YX, Wang YX, Xu XQ, Wu X, Jiang Z, He SS, et al. Occurrence and source
633 apportionment of PAHs in highly vulnerable karst system. Science of the Total
634 Environment 2014; 490: 153-160.http://doi.org/10.1016/j.scitotenv.2014.04.128.
635 Shen HZ, Huang Y, Wang R, Zhu D, Li W, Shen GF, et al. Global Atmospheric Emissions of
636 Polycyclic Aromatic Hydrocarbons from 1960 to 2008 and Future Predictions.
637 Environmental Science & Technology 2013; 47: 6415-
638 6424.http://doi.org/10.1021/es400857z.
639 Shi CH, Qu CK, Sun W, Zhou JZ, Zhang JW, Cao Y, et al. Multimedia distribution of polycyclic
640 aromatic hydrocarbons in the Wang Lake Wetland, China. Environmental Pollution
641 2022; 306.http://doi.org/10.1016/j.envpol.2022.119358.
642 Shihab K. Dynamic modeling of groundwater pollutants with Bayesian networks. Applied
643 Artificial Intelligence 2008; 22: 352-376.http://doi.org/10.1080/08839510701821645.
644 Sreedevi MA, Harikumar PS. Occurrence, distribution, and ecological risk of heavy metals and
645 persistent organic pollutants (OCPs, PCBs, and PAHs) in surface sediments of the
646 Ashtamudi wetland, south-west coast of India. Regional Studies in Marine Science
647 2023; 64.http://doi.org/10.1016/j.rsma.2023.103044.
648 Sun N, Liu J, Wang ZJ, Liu S, Wang HC, Fu Q. Phenanthrene release-migration characteristics
649 and potential influencing mechanisms from paddy soil to overlying water under
650 bioturbation in a rice-fish coculture agroecosystem. Journal of Cleaner Production
651 2023; 430.http://doi.org/10.1016/j.jclepro.2023.139719.

652 Sun T, Wang YH, Chen Y, Zhang ML, Kong XG. Occurrence of polycyclic aromatic
653 hydrocarbons in the estuarine sediments of the Taihu Lake and their associated toxic
654 effects on aquatic organisms. Pedosphere 2022; 32: 833-
655 843.http://doi.org/10.1016/j.pedsph.2022.06.021.
656 Tobiszewski M, Namiesnik J. PAH diagnostic ratios for the identification of pollution emission
657 sources. Environmental Pollution 2012; 162: 110-
658 119.http://doi.org/10.1016/j.envpol.2011.10.025.
659 Ukalska-Jaruga A, Smreczak B. The Impact of Organic Matter on Polycyclic Aromatic
660 Hydrocarbon (PAH) Availability and Persistence in Soils. Molecules 2020;
661 25.http://doi.org/10.3390/molecules25112470.
662 Wang DG, Alaee M, Byer J, Liu YJ, Tian CG. Fugacity approach to evaluate the sediment-
663 water diffusion of polycyclic aromatic hydrocarbons. Journal of Environmental
664 Monitoring 2011; 13: 1589-1596.http://doi.org/10.1039/c0em00731e.
665 Wu X, Gao XB, Tan T, Li CC, Yan RY, Chi ZY, et al. Sources and pollution path identification
666 of PAHs in karst aquifers: an example from Liulin karst water system, northern China.
667 Journal of Contaminant Hydrology 2021;
668 241.http://doi.org/10.1016/j.jconhyd.2021.103810.
669 Xiao H, Shahab A, Li JY, Xi BD, Sun XJ, He HJ, et al. Distribution, ecological risk assessment
670 and source identification of heavy metals in surface sediments of Huixian karst wetland,
671 China. Ecotoxicology and Environmental Safety 2019;
672 185.http://doi.org/10.1016/j.ecoenv.2019.109700.

673 Xiao YT, Cheng CY, Cheng AQ, Kang WH, Shen TM, Yang QR, et al. Dynamics of microbial
674 communities and organic carbon pools in karst wetland soils. Catena 2025;
675 249.http://doi.org/10.1016/j.catena.2024.108691.
676 Xie WP, Wang GJ, Yu ER, Xie J, Gong WB, Li ZF, et al. Residue character of polycyclic
677 aromatic hydrocarbons in river aquatic organisms coupled with geographic distribution,
678 feeding behavior, and human edible risk. Science of the Total Environment 2023;
679 895.http://doi.org/10.1016/j.scitotenv.2023.164814.
680 Xing X, Liu W, Li P, Su Y, Li X, Shi M, et al. Insight into the effect mechanism of sedimentary
681 record of polycyclic aromatic hydrocarbon: Isotopic evidence for lake organic matter
682 deposition and regional development model. Environ Res 2023; 239:
683 117380.http://doi.org/10.1016/j.envres.2023.117380.
684 Xing XL, Mao Y, Hu TP, Tian Q, Chen ZL, Liao T, et al. Spatial distribution, possible sources
685 and health risks of PAHs and OCPs in surface soils from Dajiuhu Sub-alpine Wetland,
686 central China. Journal of Geochemical Exploration 2020;
687 208.http://doi.org/10.1016/j.gexplo.2019.106393.
688 Xu H, Wang Q, Wang XP, Feng WH, Zhu F. Diffusion of polycyclic aromatic hydrocarbons
689 between water and sediment and their ecological risks in Wuhu city, Yangtze River
690 Delta urban agglomerations, China. Applied Geochemistry 2020;
691 119.http://doi.org/10.1016/j.apgeochem.2020.104627.
692 Xu HM, Leon JF, Liousse C, Guinot B, Yoboue V, Akpo AB, et al. Personal exposure to
693 PM_{2.5}emitted from typical anthropogenic sources in southern West

694 Africa: chemical characteristics and associated health risks. Atmospheric Chemistry
695 and Physics 2019; 19: 6637-6657.http://doi.org/10.5194/acp-19-6637-2019.
696 Yu WX, Hu LM, Zhang YY, Du JZ, Bai YZ, Lin T, et al. Sources and Fates of Sedimentary
697 Polycyclic Aromatic Hydrocarbons in the East Siberian Arctic Shelf: Implications for
698 Input Pathways and Black Carbon Constraint. Journal of Geophysical Research-
699 Oceans 2024; 129.http://doi.org/10.1029/2024jc021234.
700 Yuan HM, Li TG, Ding XG, Zhao GM, Ye SY. Distribution, sources and potential toxicological
701 significance of polycyclic aromatic hydrocarbons (PAHs) in surface soils of the Yellow
702 River Delta, China. Marine Pollution Bulletin 2014; 83: 258-
703 264.http://doi.org/10.1016/j.marpolbul.2014.03.043.
704 Yuan K, Wang XW, Lin L, Zou SC, Li Y, Yang QS, et al. Characterizing the parent and alkyl
705 polycyclic aromatic hydrocarbons in the Pearl River Estuary, Daya Bay and northern
706 South China Sea: Influence of riverine input. Environmental Pollution 2015; 199: 66-
707 72.http://doi.org/10.1016/j.envpol.2015.01.017.
708 Zhang FF, Zhang D, Lou HW, Li XY, Fu HR, Sun XJ, et al. Distribution, sources and ecological
709 risks of PAHs and n-alkanes in water and sediments of typically polluted estuaries:
710 Insights from the Xiaoqing River. Journal of Environmental Management 2024;
711 364.http://doi.org/10.1016/j.jenvman.2024.121471.
712 Zhang QX, Hu RA, Xie JX, Hu XF, Guo YD, Fang YY. Effects of microplastics on polycyclic
713 aromatic hydrocarbons migration in Baiyangdian Lake, northern China:

Concentrations, sorption-desorption behavior, and multi-phase exchange. Environmental Pollution 2025a; 366.http://doi.org/10.1016/j.envpol.2024.125408.

Zhang SZ, Xing XL, Yu HK, Du MK, Zhang Y, Li P, et al. Fate of polycyclic aromatic hydrocarbon (PAHs) in urban lakes under hydrological connectivity: A multi-media mass balance approach ☆ . Environmental Pollution 2025b; 366.http://doi.org/10.1016/j.envpol.2024.125556.

Zhang YC, Qu CK, Qi SH, Zhang Y, Mao LD, Liu JH, et al. Spatial-temporal variations and transport process of polycyclic aromatic hydrocarbons in Poyang Lake: Implication for dry-wet cycle impacts. Journal of Geochemical Exploration 2021; 226.http://doi.org/10.1016/j.gexplo.2021.106738.

Zhao ZH, Gong XH, Zhang L, Jin M, Cai YJ, Wang XL. Riverine transport and water-sediment exchange of polycyclic aromatic hydrocarbons (PAHs) along the middle-lower Yangtze River, China. Journal of Hazardous Materials 2021; 403.http://doi.org/10.1016/j.jhazmat.2020.123973.

Zhou JX, Wu QX, Gao SL, Zhang XY, Wang ZH, Wu P, et al. Coupled controls of the infiltration of rivers, urban activities and carbonate on trace elements in a karst groundwater system from Guiyang, Southwest China. Ecotoxicology and Environmental Safety 2023; 249.http://doi.org/10.1016/j.ecoenv.2022.114424.